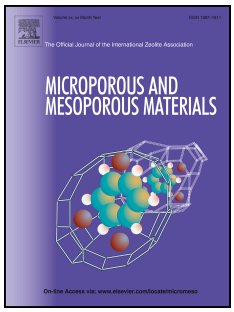

MW synthesis of ZIF-65 with a hierarchical porous structure

Vera V. Butova, Vladimir A. Polyakov, Elena A. Bulanova, Mikhail A. Soldatov, Ibrahim S. Yahia, Hebra Y. Zahran, Alla F. Abd El-Rehim, Hamed El Garni, Abdelaziz M. Aboraia, Alexander V. Soldatov

PII: S1387-1811(19)30542-6

DOI: https://doi.org/10.1016/j.micromeso.2019.109685

Reference: MICMAT 109685

To appear in: *Microporous and Mesoporous Materials*

Received Date: 11 June 2019

Revised Date: 8 August 2019

Accepted Date: 26 August 2019

Please cite this article as: V.V. Butova, V.A. Polyakov, E.A. Bulanova, M.A. Soldatov, I.S. Yahia, H.Y. Zahran, A.F. Abd El-Rehim, H. El Garni, A.M. Aboraia, A.V. Soldatov, MW synthesis of ZIF-65 with a hierarchical porous structure, *Microporous and Mesoporous Materials* (2019), doi: https://doi.org/10.1016/j.micromeso.2019.109685.

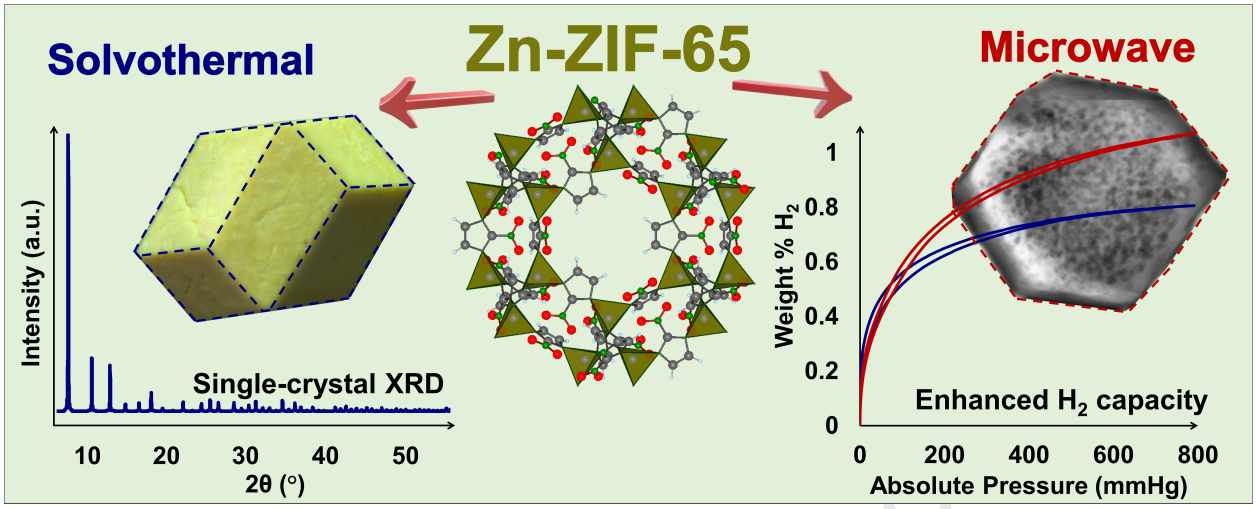

MW synthesis of ZIF-65 with a hierarchical porous structure

*Vera V. Butova**[a,b], Vladimir A. Polyakov[a,b], Elena A. Bulanova[a], Mikhail A. Soldatov[a], Ibrahim S. Yahia[c,d], Hebra Y. Zahran[c,d], Alla F. Abd El-Rehim[c,d], Hamed El Garni[d], Abdelaziz M. Aboraia[a,e], Alexander V. Soldatov[a]*

[a.] The Smart Materials Research Institute, Southern Federal University, 5 Zorge Street, Rostov-on-Don, 344090, Russian Federation.

[b.] Federal Research Centre the Southern Scientific Center of the Russian Academy of Sciences, Rostov-on-Don, Russian Federation.

[c.] Advanced Functional Materials & Optoelectronic Laboratory, Department of Physics, Faculty of Science, King Khalid University, P.O. Box 9004, Abha, Saudi Arabia.

[d.] Nanoscience Laboratory for Environmental and Bio-medical Applications (NLEBA), Semiconductor Lab., and Department of Physics, Faculty of Education, Ain Shams University, Roxy, 11757 Cairo, Egypt.

[e.] Department of Physics, Faculty of Science, Al-Azhar University, Assiut, 71542, Egypt

KEYWORDS. MOF, metal-organic framework, ZIF-8, mesopores, hydrogen storage

ABSTRACT We report two successful synthesis techniques resulted in single-phase Zn-ZIF-65 with a high specific surface area. The solvothermal method allowed to obtain large well-shaped crystals used for single-crystal XRD. We report a new MW assisted technique, which leads to a fast formation of ZIF-65 with hierarchical pore system; obtained samples contained both micro- and mesopores. Presence of micro- and mesopores was confirmed by high-resolution TEM images and analysis of nitrogen adsorption isotherm. The presence of mesopores in the micropore system is desirable for such applications as catalysis and gas storage. These additional pores lead to higher hydrogen capacity of ZIF-65 obtained using MW assisted technique.

1. Introduction

Metal-organic frameworks (MOFs) are porous materials constructed from metal clusters and organic linkers [1-3]. As these materials exhibit high specific surface areas and multifunctionality, they were successfully applied for many fields [4-8]. Most of the reported MOFs contained nanosized pore system. For some applications, like catalysis, the presence of mesopores in the micropore system is desirable, because it could decline mass transport hindrances and increase the availability of catalytic centers [9]. However, constructing of mesoporous MOFs is a challenging task due to the high probability of the structure collapse after

activation and possible interpenetrating during synthesis [10, 11]. The most obvious way for mesopores incorporating into the MOF structure is an extension of the linkers. However, it dramatically reduces stability, and only a few examples of such MOFs were reported [12-15]. The other option is defect engineering – a new strategy to tune pore size and shape [16-20]. Defects could be formed simultaneously during the synthesis or after it as a result of post-synthetic treatment [16-21].

A subclass of MOFs - Zeolitic imidazolate frameworks (ZIFs) – have attracted much scientific interest due to the exceptional stability (chemical, thermal and mechanical), tunable surface properties, and high available pore volume [22, 23]. As a result, ZIFs are attractive candidates for many applications such as separation [24, 25], gas storage and capture [26, 27], water and air decontamination [28-30], energy storage devices [31, 32], catalysis [33, 34]. ZIFs are constructed from tetrahedra $M(Im)_4$, where M stands for metal ions (e.g., Zn^{2+}, Co^{2+}), and Im is imidazolate linker. In 2010, Yaghi and coworkers reported 105 ZIFs with 38 topologies [35]. ZIF-8 is constructed from zinc ions and 2-methylimidazole linkers. The size of ZIF-8 cages is 11.6 Å with 3.4 Å windows between them [36]. Cravillon et al. reported in 2011 synthesis of ZIF-8 with n-butylamine as a modulator, which resulted in the formation of micro- and mesopores [37]. Adding of amino-acids during the synthesis of ZIF-8 in water media leads to the formation of hierarchical pores as well [38]. Combination of Zn^{2+} ions with a 2-nitroimidazole linker (NIm) results in ZIF-65 with sod topology [39] or in ZIF-77 with frl topology [36]. ZIF-65 has a 3D pore system with 10.4 Å cavities connected through 3.4 Å windows and high specific surface area 1317 m^2/g [36, 40]. Each cage includes twelve $-NO_2$ groups. Polar $-NO_2$ group in ZIF-65 framework increase affinity for CO_2 molecules in comparison with $-CH_3$ group in ZIF-8 [36, 40, 41]. ZIF-65 nanoparticles were also applied for controlled NO-release [42].

In the present work, we report on MW synthesis of ZIF-65 with hierarchical pore system. Obtained material has both micro- and mesopores. For comparison, micropore ZIF-65 was obtained using a solvothermal technique. Presence of mesopores was determined by TEM and porosity measurements. Single-crystal X-Ray diffraction was applied to determine the structure of ZIF-65 obtained by solvothermal synthesis route.

2. Experimental

2.1. Synthesis

The starting materials dimethylformamide (DMF), zinc nitrate (Zn(NO3)2·6H2O), and 2-nitroimidazole (NIm) were produced by Alfa Aesar and were used without further purification. For MW synthesis laboratory microwave system CEM Discover SP was used.

For solvothermal (ST) synthesis of ZIF-65, we used the adopted technique reported in [36]. Zinc nitrate hexahydrate and NIm were dissolved separately in DMF. Then both solutions were mixed in the glass vessel, closed and heated at 100 °C for 120 h (for details see ESI Section 1). For MW synthesis zinc nitrate hexahydrate and NIm were dissolved separately in DMF and mixed to form a clear solution (molar ratios are provided in Table 1). The reaction mixture was placed into the glass vessel, closed hermetically by silicon cap with Teflon inset and heated in MW oven for 15 minutes at 140 °C with magnetic stirring.

Table 1 Molar ratio of starting materials used for ZIF-65 synthesis and sample characterization

	The molar ratio of starting materials			Yield*, %	SSA**, m^2/g	Amount of adsorbed H_2, weight %		Cell parameter *a****, Å
	Zn^{2+}	NIm	DMF			at 20 mmHg	at 750 mmHg	
ZIF-65 ST	1	4.3	320	68 (60)	1417	0.305	0.802	17.2942(9)
ZIF-65 MW	1	4	320	67 (51)	1388	0.275	1.060	17.2719(10)

* yield according to the weight of the product is provided without parentheses, while the value in parentheses was calculated with TGA correction, according to the weight of solid product after heating in the airflow.

** SSA stands for specific surface area, calculated according to the BET model.

*** lattice constants were calculated in the program package Jana2006 according to powder XRD data.

2.2. Characterization

The phase purity of ZIF samples was determined by means of laboratory level X-ray powder diffraction (XRPD) system D2 Phaser (Bruker) operating with Cu Kαradiation (λ= 1.5418 Å). The 5-50° 2θdata range was collected at step intervals of 0.02° with 0.1 s counting time per step. Further profile analysis was done using Jana2006 software [43]. The SSA and porosity were determined by Brunauer-Emmett-Teller (BET)[44] method from the nitrogen physisorption isotherm. The sample was activated at 200 °C for 24 h in a dynamic vacuum before the measurement. Hydrogen capacity was calculated using H_2 adsorption-desorption isotherms on a sample activated at 150 °C for ten h in a dynamic vacuum. Both isotherms (N_2 and H_2) were obtained (at -196 °C) on Accelerated Surface Area and Porosimetry analyzer ASAP 2020 (Micromeritics). Total pore volume was determined using the adsorption branch of the isotherms at $P/P_0 = 0.97$. The mesopore volume was calculated from BJH adsorption cumulative volume of pores between 3.00 and 300.00 nm in diameter. The micropore volume was obtained by t-plot micropore analysis. IR spectra were measured on a Bruker Vertex 70 spectrometer in ATR (Attenuated total reflectance) geometry using an MCT detector and a Bruker Platinum ATR attachment. The spectra were measured in the range from 5000 to 300 cm^{-1} with a resolution of 1 cm^{-1} and 128 scans. The reference is air. The single-crystal X-ray experiment was carried out using a SMART APEX2 CCD diffractometer (λ(Mo-Kα) = 0.71073 Å, graphite monochromator, ω-scans) at 120 K. For the imaging of the ZIF-65 MW samples, a high-resolution transmission electron microscope (TEM), FEI Tecnai G2 F20 was employed. Sampling was done by dispersion of powders in absolute isopropanol. Thermogravimetric analysis (TGA) was performed on an STA 449 F5 Jupiter analyzer (Netzsch) with samples held in corundum pans in the flux of air with a heating rate of 10 °C/min.

3. Results and discussion

ST synthesis resulted in large crystals (0.4-1.0 mm), used for single-crystal XRD analysis, while MW-synthesis led to the yellow homogeneous powder.

XRPD patterns revealed high crystallinity of both obtained samples in good agreement with previously reported data (Figure 1a). Both profiles were indexed in cubic symmetry in I-43m space group; calculated lattice constants of both samples are very close to each other (Table 1).

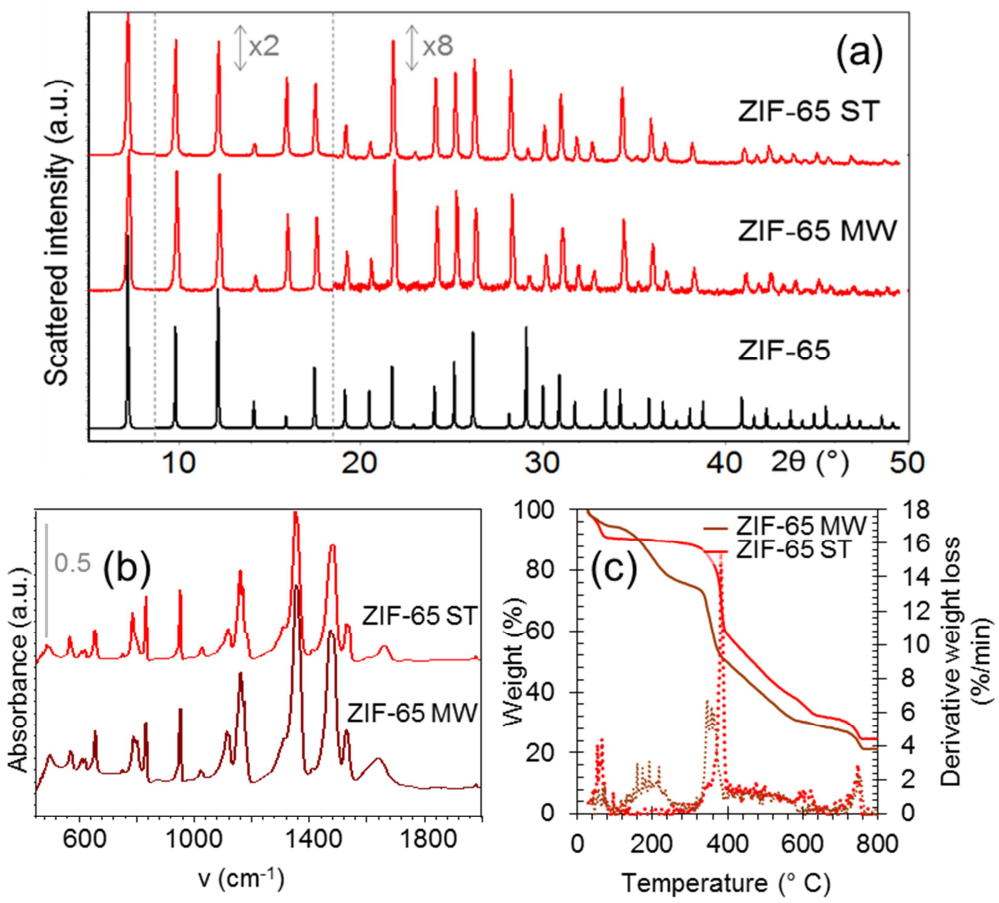

Figure 1 (a) XRPD patterns of obtained samples ZIF-65 ST and ZIF-65 MW. The black profile was calculated according to structural data for ZIF-65 (CCDC 671072). To better appreciate the higher 2θ angle data, the patterns have been multiplied by a factor 2 and 8 in the 10−15°and 15−50° 2θ-intervals. FTIR spectra (b) and TGA curves (c) of the samples ZIF-65 ST and ZIF-65 MW.

FTIR spectra of the samples ZIF-65 ST and ZIF-65 MW exhibit characteristic modes at 1360 and 1530 cm^{-1} associated with symmetric and asymmetric stretching vibrations of -NO_2 group (Figure 1b) [39, 45]. Ring out-of-plane deformation results in two modes at 614 and 656 cm^{-1}. Mode at 832 cm^{-1} is attributed to joint vibrations of aromatic C-N-C group and N-C-NO_2 group. The absorption peak of C-N stretching and C-H bending vibrations of the NIm linker was seen at 950 cm^{-1}, and aromatic C-N stretching absorption peak was observed around 1025 cm^{-1} [46]. The mode at 1660 cm^{-1} on the ZIF-65 MW spectra could be attributed to the vibrations of adsorbed DMF molecules [47]. TGA curves of synthesized samples are presented in Figure 1c. First weight loss region on the ZIF-65 ST and ZIF-65 MW curves at a temperature below 100 °C related to the evacuation of adsorbed water molecules. After it ZIF-65 ST curve exhibit long plateau, while ZIF-65 MW sample at the temperature 200 °C demonstrates the second step

associated with DMF release in good agreement with FTIR data. Heating in the airflow up to 330 °C leads to framework collapse with the formation of ZnO at 750-800 °C. Weight losses of ZIF-65 ST and ZIF-65 MW are very close to the theoretical one - 71.9% and 71.3%, respectively (Figure 1c).

The main results of the single-crystal analysis are provided in Table 2 and Section 3 of ESI. It was determined that each unit cell contain 18 disordered DMF molecules.

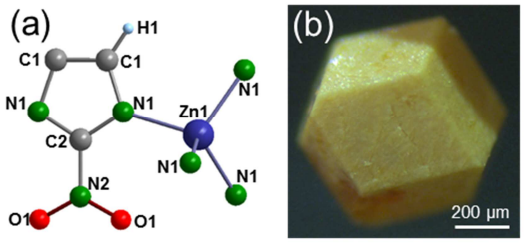

Figure 2 Designation of atomic positions in ZIF-65 (a) and photo of the crystal ZIF-65 ST obtained using an optical microscope.

Table 2 Crystal data and structure refinement for ZIF-65. Atomic coordinates ($\cdot 10^4$) and equivalent isotropic displacement parameters ($Å^2 \cdot 10^3$) for ZIF-65. U(eq) is defined as one-third of the trace of the orthogonalized U^{ij} tensor.

Empirical formula*	$C_{10.5}H_{14.5}N_{7.5}O_{5.5}Zn$		Space group	I-43m
Formula weight	399.17		Volume, $Å^3$	5170.3(4)
Unit cell dimensions, Å	17.2917(5)		Z	12
Atomic coordinates				
	x	y	z	U (eq)
Zn1	10000	2500	5000	38(1)
O1	8997(1)	3818(1)	5297(1)	66(1)
N1	10176(1)	3076(1)	6002(1)	41(1)
N2	9246(1)	4107(1)	5893(1)	47(1)
C2	9871(1)	3726(1)	6274(1)	36(1)
C1	10753(1)	2925(1)	6520(1)	61(1)

* $C_{10.5}H_{14.5}N_{7.5}O_{5.5}Zn = Zn(NIm)_2 \cdot 1.5DMF$

TEM images of ZIF-65 MW sample revealed the hexagonal shape of obtained crystals with size about 0.8-1 µm (Fig S4 in ESI). On the surface of the crystals, mesopores are well distinguishable (Figure 3). The sponge-like surface of the crystals with meso-cages detected using high magnification could be considered direct evidence of hierarchical pores in the obtained samples. As it was reported previously, MW synthesis of ZIF-8 in the same conditions leads to the microporous samples without mesopores [29, 48]. So, we suppose that the presence of NIm instead of 2-methyleimidazole (like in ZIF-8) under the MW heating strongly affected the morphology of ZIFs. The weak interaction between $-NO_2$ groups and -NH groups of

imidazole rings results in the formation of agglomerates. Apparently, MW heating leads to the fast ZIF-65 crystallization and NIm agglomerates plays the role of the nucleus.

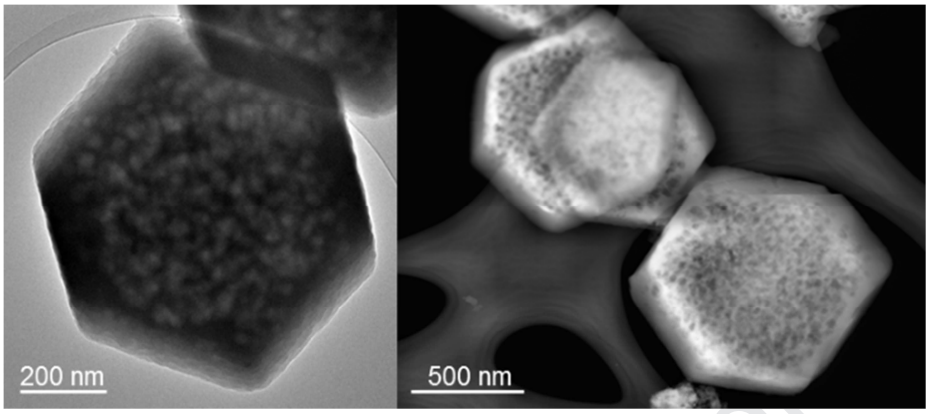

Figure 3 TEM images of ZIF-65 MW sample

Nitrogen adsorption isotherms of samples ZIF-65 ST and ZIF-65 MW are presented in Figure 4a. The isotherm of ZIF-65 ST exhibit two steps and hysteresis in good agreement with previously reported data [39]. These steps are associated with the gate-opening effect, which was already observed in ZIF-8 structure [49]. The difference in the shape of isotherms between ZIF-8 and ZIF-65 ST could be attributed to different functional groups in the linkers. It was reported that under the pressure ZIF-8 structure firstly open six-member windows, while ZIF-65 – four-member windows [50].

As it was reported previously applying of BJH method for mesoporous analysis leads to underestimation the pore size by as much as 30%, while methods based on molecular simulation, such as DFT, can describe the adsorption accurately, to the molecular level, because they give thermodynamic and density profiles of confined fluids in pores [51]. So, the pore size distribution was calculated according to the model of slit pores by original DFT method. Sample ZIF-65 MW indicates the presence of mesopores in 3-7 nm range and micropores about 0.8-1.0 nm, while the same diagram in the case of ZIF-65 ST sample exhibit only micropores about 0.7-0.9 nm. This data is in good agreement with pore volume calculations. Micropore volumes of both samples are very close (ZIF-65 ST – 0.47 cm^3/g, ZIF-65 MW – 0.42 cm^3/g), while in mesopores range samples demonstrate significant difference (ZIF-65 ST – 0.04 cm^3/g, ZIF-65 MW – 0.57 cm^3/g). As a result, the total pore volume of sample ZIF-65 MW (0.91 cm^3/g) almost twice higher than the one of sample ZIF-65 ST (0.55 cm^3/g).

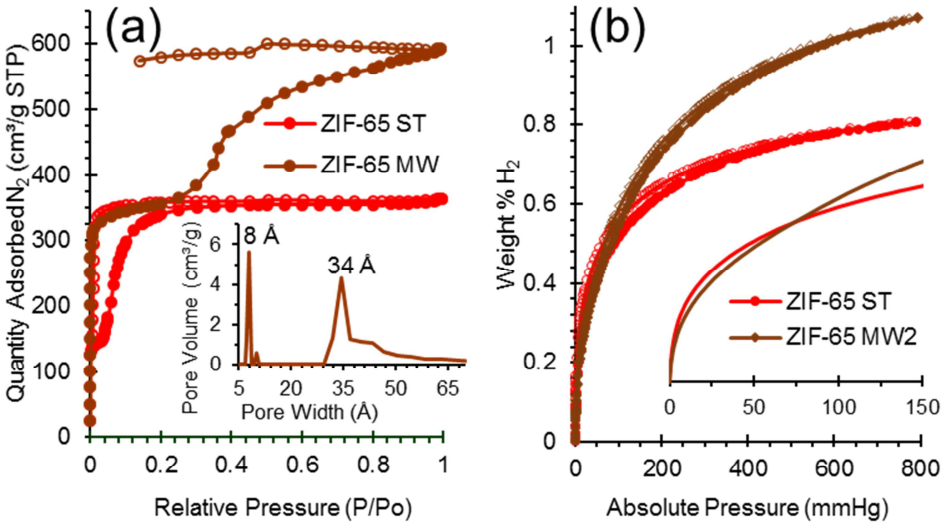

Figure 4 Nitrogen (a) and hydrogen (b) adsorption isotherms of samples ZIF-65 ST (red lines) and ZIF-65 MW (brown lines). Full markers represent adsorption branches of isotherms, while empty ones – desorption branches. Inset in part (a) exhibit pore size distribution, calculated using Original Density Functional Theory according to the model of slit pores. Inset in part (b) shows adsorption branches in low-pressure region 0-150 mmHg.

Both samples were also tested for hydrogen sorption (Figure 4b). As it follows from the presented isotherms at the low-pressure region below 70 mmHg ZIF-65 ST exhibit higher H_2 capacity, while at the pressures higher than 70 mmHg ZIF-65 MW adsorb more H_2, and this trend becomes more pronounced with an increase of pressure. These observations are in good agreement with the formation of hierarchical pores in ZIF-65 MW sample and with previously reported data. Small pores play a significant role in adsorbing hydrogen at low pressures, while the large cages in these conditions proved far less efficient. However, for mesoporous materials at high pressure, the pore volume controls H_2 loadings [8, 10]. So, in the case of ZIF-65 samples, at low pressures, hydrogen fills micropores, which are preferable for small H_2 molecules. At higher pressures sample ZIF-65 MW could provide additional space in mesopores, while ZIF-65 ST does not contain them, and adsorption branch of hydrogen isotherm reaches plateau region.

4. Conclusions

We have reported two successful synthesis methods – solvothermal and microwave-assisted, which are result in single-phase ZIF-65 material with a high specific surface area. Solvothermal conditions allow slow crystal growth, and it leads to the formation of large well-shaped crystals. MW heating provides fast heat transfer, which results in sub-micron ZIF-65 particles with hierarchical pore system. The sample obtained using an MW oven contained both micro- and mesopores. It was confirmed by nitrogen sorption measurements and, moreover, it could be directly observed on TEM images of the crystals. This hierarchical pore system is promising for many applications, like catalysis. The other feature of the reported synthesis technique is the absence of any additives. As we did not use any modulators or alkali agents, the surface of the defect pores is not decorated with any compensative chemicals. It simplifies post-synthetic

washing and activation procedures. Presence of mesopores in obtained ZIF-65 was confirmed by N2 adsorption m We have tested both materials for hydrogen storage and revealed a higher H_2 capacity of the sample with mesopores. Micropores are preferable for hydrogen adsorption, and at low pressures, both samples (with only micropores and with both micro- and mesopores) adsorb H_2 in the same way. However, when ZIF-65 ST filled all micropores and came to the plateau region, ZIF-65 MW with mesopores provided additional space for hydrogen and exhibited higher H_2 capacity.

ACKNOWLEDGMENT

The authors express their appreciation to the Deanship of Scientific Research at King Khalid University for funding this work through research groups program under grant number R.G.P.2/43/40. MAS and AVS acknowledge RFBR for financial support according to the project № 18-52-53046.

AUTHOR INFORMATION

Corresponding Author

Vera V. Butova. e-mail VButova@sfedu.ru, 344090 Zorge 5, Rostov-on-Don, Russia

REFERENCES

[1] O.M. Yaghi, M. O'Keeffe, N.W. Ockwig, H.K. Chae, M. Eddaoudi, J. Kim, Reticular synthesis and the design of new materials, Nature, 423 (2003) 705-714.
[2] D.J. Tranchemontagne, J.L. Mendoza-Cortes, M. O'Keeffe, O.M. Yaghi, Secondary building units, nets and bonding in the chemistry of metal-organic frameworks, Chem. Soc. Rev., 38 (2009) 1257-1283.
[3] V.V. Butova, M.A. Soldatov, A.A. Guda, K.A. Lomachenko, C. Lamberti, Metal-organic frameworks: structure, properties, methods of synthesis and characterization, Russ. Chem. Rev., 85 (2016) 280-307.
[4] M. Ranocchiari, J.A. van Bokhoven, Catalysis by metal-organic frameworks: fundamentals and opportunities, Phys. Chem. Chem. Phys., 13 (2011) 6388-6396.
[5] N.L. Rosi, J. Eckert, M. Eddaoudi, D.T. Vodak, J. Kim, M. O'Keeffe, O.M. Yaghi, Hydrogen storage in microporous metal-organic frameworks, Science, 300 (2003) 1127-1129.
[6] L.J. Murray, M. Dinca, J.R. Long, Hydrogen storage in metal-organic frameworks, Chem. Soc. Rev., 38 (2009) 1294-1314.
[7] S. Chavan, J.G. Vitillo, D. Gianolio, O. Zavorotynska, B. Civalleri, S. Jakobsen, M.H. Nilsen, L. Valenzano, C. Lamberti, K.P. Lillerud, S. Bordiga, H-2 storage in isostructural UiO-67 and UiO-66 MOFs, Phys. Chem. Chem. Phys., 14 (2012) 1614-1626.
[8] V.V. Butova, A.P. Budnyk, K.M. Charykov, K.S. Vetlitsyna-Novikova, A.L. Bugaev, A.A. Guda, A. Damin, S.M. Chavan, S. Øien-ØDegaard, K.P. Lillerud, A.V. Soldatov, C. Lamberti, Partial and Complete Substitution of the 1,4-Benzenedicarboxylate Linker in UiO-66 with 1,4-Naphthalenedicarboxylate: Synthesis, Characterization, and H2-Adsorption Properties, Inorg. Chem., 58 (2019) 1607-1620.
[9] W.L. Xu, K.B. Thapa, Q. Ju, Z.L. Fang, W. Huang, Heterogeneous catalysts based on mesoporous metal-organic frameworks, Coord. Chem. Rev., 373 (2018) 199-232.
[10] L.F. Song, J. Zhang, L.X. Sun, F. Xu, F. Li, H.Z. Zhang, X.L. Si, C.L. Jiao, Z.B. Li, S. Liu, Y.L. Liu, H.Y. Zhou, D.L. Sun, Y. Du, Z. Cao, Z. Gabelica, Mesoporous metal-organic frameworks: design and applications, Energy Environ. Sci., 5 (2012) 7508-7520.

[11] T.H. Chen, I. Popov, Y.C. Chuang, Y.S. Chen, O.S. Miljanic, A mesoporous metal-organic framework based on a shape-persistent macrocycle, Chem. Commun., 51 (2015) 6340-6342.
[12] G. Ferey, C. Mellot-Draznieks, C. Serre, F. Millange, J. Dutour, S. Surble, I. Margiolaki, A chromium terephthalate-based solid with unusually large pore volumes and surface area, Science, 309 (2005) 2040-2042.
[13] D.Q. Yuan, D. Zhao, D.F. Sun, H.C. Zhou, An Isoreticular Series of Metal-Organic Frameworks with Dendritic Hexacarboxylate Ligands and Exceptionally High Gas-Uptake Capacity, Angew. Chem.-Int. Edit., 49 (2010) 5357-5361.
[14] X. Lin, I. Telepeni, A.J. Blake, A. Dailly, C.M. Brown, J.M. Simmons, M. Zoppi, G.S. Walker, K.M. Thomas, T.J. Mays, P. Hubberstey, N.R. Champness, M. Schroder, High Capacity Hydrogen Adsorption in Cu(II) Tetracarboxylate Framework Materials: The Role of Pore Size, Ligand Functionalization, and Exposed Metal Sites, J. Am. Chem. Soc., 131 (2009) 2159-2171.
[15] L.Q. Ma, J.M. Falkowski, C. Abney, W.B. Lin, A series of isoreticular chiral metal-organic frameworks as a tunable platform for asymmetric catalysis, Nat. Chem., 2 (2010) 838-846.
[16] U. Ravon, M. Savonnet, S. Aguado, M.E. Domine, E. Janneau, D. Farrusseng, Engineering of coordination polymers for shape selective alkylation of large aromatics and the role of defects, Microporous Mesoporous Mat., 129 (2010) 319-329.
[17] G.C. Shearer, S. Chavan, S. Bordiga, S. Svelle, U. Olsbye, K.P. Lillerud, Defect Engineering: Tuning the Porosity and Composition of the Metal-Organic Framework UiO-66 via Modulated Synthesis, Chem. Mat., 28 (2016) 3749-3761.
[18] G.C. Shearer, J.G. Vitillo, S. Bordiga, S. Svelle, U. Olsbye, K.P. Lillerud, Functionalizing the Defects: Postsynthetic Ligand Exchange in the Metal Organic Framework UiO-66, Chem. Mat., 28 (2016) 7190-7193.
[19] C. Atzori, G.C. Shearer, L. Maschio, B. Civalleri, F. Bonino, C. Lamberti, S. Svelle, K.P. Lillerud, S. Bordiga, Effect of Benzoic Acid as a Modulator in the Structure of UiO-66: An Experimental and Computational Study, J. Phys. Chem. C, 121 (2017) 9312-9324.
[20] V.V. Butova, A.P. Budnyk, A.A. Guda, K.A. Lomachenko, A.L. Bugaev, A.V. Soldatov, S.M. Chavan, S. Oien-Odegaard, U. Olsbye, K.P. Lillerud, C. Atzori, S. Bordiga, C. Lamberti, Modulator Effect in UiO-66-NDC (1,4-Naphthalenedicarboxylic Acid) Synthesis and Comparison with UiO-67-NDC Isoreticular Metal-Organic Frameworks, Cryst. Growth Des., 17 (2017) 5422-5431.
[21] F. Vermoortele, R. Ameloot, L. Alaerts, R. Matthessen, B. Carlier, E.V.R. Fernandez, J. Gascon, F. Kapteijn, D.E. De Vos, Tuning the catalytic performance of metal-organic frameworks in fine chemistry by active site engineering, J. Mater. Chem., 22 (2012) 10313-10321.
[22] K.S. Park, Z. Ni, A.P. Cote, J.Y. Choi, R.D. Huang, F.J. Uribe-Romo, H.K. Chae, M. O'Keeffe, O.M. Yaghi, Exceptional chemical and thermal stability of zeolitic imidazolate frameworks, Proc. Natl. Acad. Sci. U. S. A., 103 (2006) 10186-10191.
[23] Y.V. Kaneti, S. Dutta, M.S.A. Hossain, M.J.A. Shiddiky, K.L. Tung, F.K. Shieh, C.K. Tsung, K.C.W. Wu, Y. Yamauchi, Strategies for Improving the Functionality of Zeolitic Imidazolate Frameworks: Tailoring Nanoarchitectures for Functional Applications, Adv. Mater., 29 (2017).
[24] J.F. Yao, H.T. Wang, Zeolitic imidazolate framework composite membranes and thin films: synthesis and applications, Chem. Soc. Rev., 43 (2014) 4470-4493.
[25] W.H. Yuan, X.T. Zhang, L. Li, Synthesis of zeolitic imidazolate framework-69 for adsorption separation of ethane and ethylene, J. Solid State Chem., 251 (2017) 198-203.
[26] A.G. Kontos, V. Likodimos, C.M. Veziri, E. Kouvelos, N. Moustakas, G.N. Karanikolos, G.E. Romanos, P. Falaras, CO2 Captured in Zeolitic Imidazolate Frameworks: Raman

Spectroscopic Analysis of Uptake and Host-Guest Interactions, ChemSusChem, 7 (2014) 1696-1702.
[27] T. Pham, K.A. Forrest, H. Furukawa, M. Russina, A. Albinati, P.A. Georgiev, J. Eckert, B. Space, High H-2 Sorption Energetics in Zeolitic Imidazolate Frameworks, J. Phys. Chem. C, 121 (2017) 1723-1733.
[28] G.D. Fan, R.J. Lin, Z.Y. Su, R.X. Xu, Removing Water Contaminants Using Zeolitic Imidazolate Frameworks, Prog. Chem., 28 (2016) 1753-1761.
[29] V.V. Butova, V.A. Polyakov, A.P. Budnyk, A.M. Aboraia, E.A. Bulanova, A.A. Guda, E.A. Reshetnikova, Y.S. Podkovyrina, C. Lamberti, A.V. Soldatov, Zn/Co ZIF family: MW synthesis, characterization and stability upon halogen sorption, Polyhedron, 154 (2018) 457-464.
[30] V.V. Butova, E.A. Bulanova, V.A. Polyakov, A.A. Guda, A.M. Aboraia, V.V. Shapovalov, H.Y. Zahran, I.S. Yahia, A.V. Soldatov, The effect of cobalt content in Zn/Co-ZIF-8 on iodine capping properties, Inorg. Chim. Acta, 492 (2019) 18-22.
[31] X.L. Xu, H. Wang, J.B. Liu, H. Yan, The applications of zeolitic imidazolate framework-8 in electrical energy storage devices: a review, J. Mater. Sci.-Mater. Electron., 28 (2017) 7532-7543.
[32] S. Dutta, Z. Liu, H. Han, A. Indra, T. Song, Electrochemical Energy Conversion and Storage with Zeolitic Imidazolate Framework Derived Materials: A Perspective, ChemElectroChem, 5 (2018) 3571-3588.
[33] A. Zanon, F. Verpoort, Metals@ZIFs: Catalytic applications and size selective catalysis, Coord. Chem. Rev., 353 (2017) 201-222.
[34] G.H. Zhong, D.X. Liu, J.Y. Zhang, The application of ZIF-67 and its derivatives: adsorption, separation, electrochemistry and catalysts, J. Mater. Chem. A, 6 (2018) 1887-1899.
[35] A. Phan, C.J. Doonan, F.J. Uribe-Romo, C.B. Knobler, M. O'Keeffe, O.M. Yaghi, Synthesis, Structure, and Carbon Dioxide Capture Properties of Zeolitic Imidazolate Frameworks, Accounts Chem. Res., 43 (2010) 58-67.
[36] R. Banerjee, A. Phan, B. Wang, C. Knobler, H. Furukawa, M. O'Keeffe, O.M. Yaghi, High-throughput synthesis of zeolitic imidazolate frameworks and application to CO2 capture, Science, 319 (2008) 939-943.
[37] J. Cravillon, R. Nayuk, S. Springer, A. Feldhoff, K. Huber, M. Wiebcke, Controlling Zeolitic Imidazolate Framework Nano- and Microcrystal Formation: Insight into Crystal Growth by Time-Resolved In Situ Static Light Scattering, Chem. Mat., 23 (2011) 2130-2141.
[38] Y.N. Wu, M.M. Zhou, B.R. Zhang, B.Z. Wu, J. Li, J.L. Qiao, X.H. Guan, F.T. Li, Amino acid assisted templating synthesis of hierarchical zeolitic imidazolate framework-8 for efficient arsenate removal, Nanoscale, 6 (2014) 1105-1112.
[39] M. Tu, C. Wiktor, C. Rosler, R.A. Fischer, Rapid room temperature syntheses of zeolitic-imidazolate framework (ZIF) nanocrystals, Chem. Commun., 50 (2014) 13258-13260.
[40] E. Atci, S. Keskin, Atomically Detailed Models for Transport of Gas Mixtures in ZIF Membranes and ZIF/Polymer Composite Membranes, Ind. Eng. Chem. Res., 51 (2012) 3091-3100.
[41] G. Yilmaz, S. Keskin, Predicting the Performance of Zeolite Imidazolate Framework/Polymer Mixed Matrix Membranes for CO2, CH4, and H-2 Separations Using Molecular Simulations, Ind. Eng. Chem. Res., 51 (2012) 14218-14228.
[42] S. Diring, D.O. Wang, C. Kim, M. Kondo, Y. Chen, S. Kitagawa, K. Kamei, S. Furukawa, Localized cell stimulation by nitric oxide using a photoactive porous coordination polymer platform, Nat. Commun., 4 (2013).
[43] V. Petříček, M. Dušek, L. Palatinus, Crystallographic Computing System JANA2006: General features, Z. Kristallog., 229 (2014) 345-352.

[44] S. Brunauer, P.H. Emmett, E. Teller, Adsorption of Gases in Multimolecular Layers, J. Am. Chem. Soc., 60 (1938) 309-319.
[45] M. Tu, S. Wannapaiboon, K. Khaletskaya, R.A. Fischer, Engineering Zeolitic-Imidazolate Framework (ZIF) Thin Film Devices for Selective Detection of Volatile Organic Compounds, Adv. Funct. Mater., 25 (2015) 4470-4479.
[46] V. Arjunan, P. Ravindran, R. Santhanam, A. Raj, S. Mohan, A comparative study on vibrational, conformational and electronic structure of 1,2-dimethyl-5-nitroimidazole and 2-methyl-5-nitroimidazole, Spectrochimica Acta Part A: Molecular and Biomolecular Spectroscopy, 97 (2012) 176-188.
[47] X.B. Cao, L.L. Zhi, Y.H. Li, F. Fang, X. Cui, Y.W. Yao, L.J. Ci, K.X. Ding, J.Q. Wei, Elucidating the Key Role of a Lewis Base Solvent in the Formation of Perovskite Films Fabricated from the Lewis Adduct Approach, ACS Appl. Mater. Interfaces, 9 (2017) 32868-32875.
[48] V.V. Butova, A.P. Budnik, E.A. Bulanova, A.V. Soldatov, New microwave-assisted synthesis of ZIF-8, Mendeleev Commun., 26 (2016) 43-44.
[49] D. Fairen-Jimenez, S.A. Moggach, M.T. Wharmby, P.A. Wright, S. Parsons, T. Duren, Opening the Gate: Framework Flexibility in ZIF-8 Explored by Experiments and Simulations, J. Am. Chem. Soc., 133 (2011) 8900-8902.
[50] C.L. Hobday, T.D. Bennett, D. Fairen-Jimenez, A.J. Graham, C.A. Morrison, D.R. Allan, T. Duren, S.A. Moggach, Tuning the Swing Effect by Chemical Functionalization of Zeolitic Imidazolate Frameworks, J. Am. Chem. Soc., 140 (2018) 382-387.
[51] M. Thommes, K. Kaneko, A.V. Neimark, J.P. Olivier, F. Rodriguez-Reinoso, J. Rouquerol, K.S.W. Sing, Physisorption of gases, with special reference to the evaluation of surface area and pore size distribution (IUPAC Technical Report), Pure Appl. Chem., 87 (2015) 1051-1069.

Highlights

for

MW synthesis of ZIF-65 with a hierarchical porous structure

Vera V. Butova[*a,b], Vladimir A. Polyakov[a,b], Elena A. Bulanova[a], Mikhail A. Soldatov[a], Ibrahim S. Yahia[c,d], Hebra Y. Zahran[c,d], Alla F. Abd El-Rehim[c,d], Hamed El Garni[d], Abdelaziz M. Aboraia[a,e], Alexander V. Soldatov[a]*

[a.] The Smart Materials Research Institute, Southern Federal University, 5 Zorge Street, Rostov-on-Don, 344090, Russian Federation.

[b.] Federal Research Centre the Southern Scientific Center of the Russian Academy of Sciences, Rostov-on-Don, Russian Federation.

[c.] Advanced Functional Materials & Optoelectronic Laboratory, Department of Physics, Faculty of Science, King Khalid University, P.O. Box 9004, Abha, Saudi Arabia.

[d.] Nanoscience Laboratory for Environmental and Bio-medical Applications (NLEBA), Semiconductor Lab., and Department of Physics, Faculty of Education, Ain Shams University, Roxy, 11757 Cairo, Egypt.

[e.] Department of Physics, Faculty of Science, Al-Azhar University, Assiut, 71542, Egypt

- New microwave-assisted synthesis of ZIF-65 with hierarchical pore system
- Obtained samples contain both micro- and mesopores
- Additional pores lead to higher hydrogen capacity
- ZIF-65 with micropores was obtained using a solvothermal technique
- Large well-shaped crystals were used for single-crystal XRD